



ELSEVIER

Contents lists available at ScienceDirect

Journal of Ginseng Research

journal homepage: <https://www.sciencedirect.com/journal/journal-of-ginseng-research>

Research Article

Ginsenosides repair UVB-induced skin barrier damage in BALB/c hairless mice and HaCaT keratinocytes

Zhenzhuo Li ^{a, b, 1}, Rui Jiang ^{b, 1}, Manying Wang ^{a, b}, Lu Zhai ^b, Jianzeng Liu ^a, Xiaohao Xu ^b, Liwei Sun ^{b, c, d, **}, Daqing Zhao ^{a, c, *}^a Jilin Ginseng Academy, Changchun University of Chinese Medicine, Changchun, Jilin, China^b Research Center of Traditional Chinese Medicine, the Affiliated Hospital to Changchun University of Chinese Medicine, Changchun, Jilin, China^c Key Laboratory of Active Substances and Biological Mechanisms of Ginseng Efficacy, Ministry of Education, Changchun University of Chinese Medicine, Changchun, Jilin, China^d Jilin Province Traditional Chinese Medicine Characteristic Health Product Research and Development Cross-regional Cooperation Science and Technology Innovation Center, Changchun University of Chinese Medicine, Changchun, Jilin, China

ARTICLE INFO

Article history:

Received 12 November 2020

Received in revised form

23 April 2021

Accepted 4 May 2021

Available online 10 May 2021

Keywords:

ginsenosides
skin barrier damage
cornified envelope
tight junctions
AQP-3

ABSTRACT

Background: Ginsenosides (GS) have potential value as cosmetic additives for prevention of skin photoaging. However, their protective mechanisms against skin barrier damage and their active monomeric constituents are unknown.**Methods:** GS monomer types and their relative proportions were identified. A UVB-irradiated BALB/c hairless mouse model was used to assess protective effects of GS components on skin epidermal thickness and transepidermal water loss (TEWL). Skin barrier function, reflected by filaggrin (FLG), involucrin (IVL), claudin-1 (Cldn-1), and aquaporin 3 (AQP3) levels and MAPK phosphorylation patterns, were analyzed in UVB-irradiated hairless mice or HaCaT cells.**Results:** Total GS monomeric content detected by UPLC was 85.45% and was largely attributed to 17 main monomers that included Re (16.73%), Rd (13.36%), and Rg1 (13.38%). In hairless mice, GS ameliorated UVB-induced epidermal barrier dysfunction manifesting as increased epidermal thickness, increased TEWL, and decreased stratum corneum water content without weight change. Furthermore, GS treatment of UVB-irradiated mice restored protein expression levels and epidermal tissue distributions of FLG, IVL, Cldn-1, and AQP3, with consistent mRNA and protein expression results obtained in UVB-irradiated HaCaT cells (except for unchanging Cldn-1 expression). Mechanistically, GS inhibited JNK, p38, and ERK phosphorylation in UVB-irradiated HaCaT cells, with a mixture of Rg2, Rg3, Rk3, F2, Rd, and Rb3 providing the same protective MAPK pathway inhibition-associated upregulation of IVL and AQP3 expression as provided by intact GS treatment.**Conclusion:** GS protection against UVB-irradiated skin barrier damage depends on activities of six ginsenoside monomeric constituents that inhibit the MAPK signaling pathway.© 2021 The Korean Society of Ginseng. Publishing services by Elsevier B.V. This is an open access article under the CC BY-NC-ND license (<http://creativecommons.org/licenses/by-nc-nd/4.0/>).

* Corresponding author. Jilin Ginseng Academy, Changchun University of Chinese Medicine, Changchun, Jilin Province, China.

** Corresponding author. Research Center of Traditional Chinese Medicine, the Affiliated Hospital to Changchun University of Chinese Medicine, Changchun, Jilin Province, China.

E-mail addresses: sunnylilwei@163.com (L. Sun), zhaodaqing1963@163.com (D. Zhao).¹ These authors contributed equally to this work.

1. Introduction

The skin barrier, mainly comprised of the epidermis, provides a physical barrier against pathogens, irritants, and UV radiation and prevents loss of water and solutes while maintaining homeostasis. The clinical appearance of UVB-induced skin barrier destruction is characterized by skin dryness, desquamation, and a rough-textured surface [1] that are experimentally associated with increased transepidermal water loss (TEWL) and increased epidermal thickness [2,3]. These changes are mainly due to damage to two mechanical barriers, the cornified envelope (CE) of the stratum

corneum (SC) and the tight junctions (TJs) of the stratum granulosum [4].

The cornified envelope encloses corneocytes that account for its role in maintaining SC structural and mechanical integrity. CE function depends on interactions among transglutaminase-crosslinked proteins, such as filaggrin (FLG) or involucrin (IVL) [5,6]. Meanwhile, TJs are complex cell-cell junctions that mainly function to seal the paracellular pathway to restrict movement of molecules within the intercellular space [7]. TJs contain the transmembrane protein claudin-1 (Cldn-1), a protein that directly interacts with proteins of the cytoplasmic plaque [4,8]. Skin barrier damage leads to drying and dehydration of skin that can be mainly counteracted by the function of aquaporin 3 (AQP3), the most abundant aquaporin found in skin. AQP3 provides a channel for the movement of moisture between the stratum basale and the stratum corneum to maintain constant moisture content within the epidermis [9]. Notably, a previous study demonstrated that UVB irradiation could stimulate MAPKs by activating phosphorylation of c-Jun N-terminal kinase (JNK), p38, and extracellular signal-regulated kinase (ERK) to ultimately alter expression levels and localization of skin barrier proteins such as FLG and AQP3 [9–12]. Therefore, maintenance of CE, TJs, and AQP3 protein functions depends on MAPK signaling pathways to ultimately achieve relief of skin dryness and desquamation.

As the main active component of *Panax ginseng* Meyer, ginsenosides (GS) have potential applications as cosmetic additives for preventing skin photoaging [13–15]. Indeed, previous reports have indicated that Re can enhance CE formation and upregulate FLG and caspase 14 activities within HaCaT keratinocytes [16], and compound K, a secondary ginsenoside derived from Rb1, also shows to augment gene expression of FLG in HaCaT cells [17]. Meanwhile, Rc enhances caspase 14 activity and upregulates FLG protein expression in a keratinocyte photooxidation damage model [18], while daily oral Rg1 intake can reduce basal TEWL from back skin of hairless mice to alleviate UV-induced aging [19]. However, the GS protective effect against UVB-induced skin barrier damage, an important cause of skin damage, and active components underlying GS protection have not yet been reported. Therefore, in this study we investigated effects of GS on UVB-induced skin barrier damage in BALB/c hairless mice and HaCaT keratinocytes and identified main bioactive ginsenoside monomers. These results provide a theoretical basis for identifying GS active components and for determining the mechanism underlying *P. ginseng* protection against skin barrier damage.

2. Materials and methods

2.1. Chemicals and reagents

Total ginsenosides (GS) from *P. ginseng* roots were isolated in our laboratory. Standard ginsenosides, including Rg1, Re, Rf, Rg2, Rh1(R), Rb1, Rc, F1, Rb2, Rb3, Rd, F2, Rk3, Rg3, PPT, Rh2(S), and PPD, each of > 98% purity, were purchased from Shanghai Yuanye Biotechnology (Shanghai, China). Dulbecco's Modified Eagle Medium (DMEM) was obtained from Thermo Fisher Scientific (Carlsbad, CA, USA). Fetal bovine serum was purchased from Clark Bioscience (Claymont, DE, USA). Penicillin and streptomycin were obtained from Biosharp (Hefei, China). MTT, retinoic acid, and DAPI were purchased from Sigma-Aldrich (St. Louis, MO, USA). TRIZOL reagent was purchased from TIANGEN (Beijing, China) and PrimeScript RT reagent kit was purchased from TaKaRa (Dalian, China). RIPA lysis buffer and BCA protein assay kit were obtained from Beyotime Biotechnology (Jiangsu, China). Protease and phosphatase inhibitors were purchased from Roche (Basel, Switzerland). PVDF membranes were obtained from GE Healthcare (Bensalem, PA,

USA). Monoclonal primary antibodies against p-JNK, JNK, p-p38, p38, p-ERK, ERK, and GAPDH were purchased from Cell Signaling Technology (Beverly, CA, USA). Anti-AQP3 polyclonal antibody was purchased from Abcam (Cambridge, MA, USA). Monoclonal primary antibodies against FLG, IVL, and Cldn-1 and enhanced chemiluminescence reagent were purchased from Santa Cruz Biotechnology (Santa Cruz, CA, USA).

2.2. Ultra-performance liquid chromatography (UPLC) analysis of GS

Chromatographic analysis was performed using a 1290 Infinity II (Agilent, USA) equipped with a Kromasil C18 column (2.5 μ m, 2.1 \times 50 mm; Kromasil, Sweden) with UV detection at 203 nm. A stepwise elution gradient was employed using solvent A (water) and solvent B (acetonitrile) and maintained at 35 °C. The gradient elution program was as follows: 18–30% B at 0–20 min, 30–50.9% B at 20–31 min, 50.9–65% B at 31–36 min, 65–18% B at 36–40 min. The flow rate was 0.3 mL/min and the sample injection volume was 6 μ L.

2.3. Animals

Six-week-old female BALB/c hairless mice were purchased from Changchun Yisi Animal Feeding Center (Jilin, China). Before they were used in experiments, mice were permitted to acclimate for one week in a temperature- and humidity-controlled facility (22 \pm 1 °C and 55 \pm 5% relative humidity) with 12 h/12 h light/dark cycle. Food and water were supplied *ad libitum*. All experimental procedures for animal experiments were reviewed and approved by the Animal Ethics Committee of Changchun University of Chinese Medicine (Jilin, China).

2.4. UVB irradiation and treatments

After a week of acclimatization, mice were randomly divided into four groups (5 mice/group): control group (no UVB irradiation), UVB-irradiated group, UVB + Vehicle group (20% propylene glycol), and UVB + GS treatment group (2.0 mg/cm²/day in 20% propylene glycol). Hairless mice were exposed to UVB irradiation at a dose of 100 mJ/cm² per day for the first two days and 150 mJ/cm² per day for the next two days using a UV crosslinker system (Hofer Scientific Instruments, San Francisco, CA, USA) with an emission wavelength peak of 312 nm. Subsequently, the dose was increased to 200 mJ/cm² on the 5th day until the experiment was completed on the 14th day (Fig. 2B). The control group was given a normal diet and water, while the UV-irradiated group was exposed to UVB light for 2 weeks. Skin of mice in the UVB + Vehicle group was smeared with 2.0 mg/cm² of 20% propylene glycol after UVB irradiation. In the UVB + GS treatment group, GS was applied to the exposed skin areas on the backs of the mice at a concentration of 2.0 mg/cm² per day after daily exposure to UVB light. After each day of treatment, body weights of mice in each group were measured.

2.5. Measurement of TEWL and stratum corneum water content

A Tewameter (TM300) and a Corneometer (CM825, Courage & Khazaka, Cologne, Germany) were used to measure TEWL and stratum corneum water content of the dorsal skin of hairless mice, respectively. TEWL and stratum corneum water content values were automatically calculated and expressed as g/m²h and arbitrary units (AU). These measurements were carried out at 21–22 °C and 50–55% humidity and measured after 0 and 14 days of GS treatment.

2.6. Histopathology

At completion of the experimental course, skin tissues were fixed in 4% paraformaldehyde for 24 h, dehydrated in ethanol, then embedded in paraffin. Sliced sections of 3- μ m thickness were stained with hematoxylin and eosin (H&E) then samples were examined under an Olympus microscope (TH4-200, Tokyo, Japan). Histomorphometric analyses were performed to determine epithelial thickness (μ m) using Gen 5 data analysis software (Bio-Tek, Winooski, VT, USA).

2.7. Immunohistochemistry

Skin samples were cut into 3- μ m thick sections, deparaffinized, rehydrated, and sectioned as described previously [20]. The sections were incubated in endogenous peroxidase blocking solution for 10 min then non-specific binding of proteins was blocked with normal non-immune serum for 10 min. After incubation with primary antibodies for 1 h, the sections were treated with biotin-conjugated secondary antibody and freshly prepared DAB solution (Santa Clara, CA, USA) then were counterstained with hematoxylin. The immunostained sections were observed under an M8 microscope (PreciPoint GmbH, Freising, Germany).

2.8. Western blot analysis

Skin tissues and cells were lysed with RIPA lysis buffer supplemented with protease and phosphatase inhibitors. Protein concentrations were measured using a BCA protein assay kit. Protein samples (50 μ g) were separated by 12% SDS-PAGE gels then were transferred to PVDF membranes. After blocking with 5% fat-free milk, membranes were incubated with primary antibodies (1:1000) overnight at 4 °C followed by incubation with appropriate secondary antibodies (1:5000) for 1 h. Next, transferred protein bands were visualized and analyzed using the chemiluminescence imaging system (FluorChem HD2; ProteinSimple, San Jose, CA, USA).

2.9. Cell culture and treatments

Human epidermal keratinocyte (HaCaT) cells were purchased from Shanghai Fuheng Biotechnology Co., Ltd. (Shanghai, China) and were maintained in DMEM supplemented with 10% fetal bovine serum, 100 units/mL penicillin, and 100 μ g/mL streptomycin in an incubator with a 37 °C humidified atmosphere containing 5% CO₂. HaCaT cells (3×10^5 cells/well) were irradiated in 35-mm diameter cell culture dishes. Before UVB irradiation, the culture medium was replaced with 1 mL of phosphate-buffered saline (PBS) per well. The cells were irradiated at 40 mJ/cm² in uncovered plastic culture dishes. After UVB irradiation, the PBS was removed and cells were treated with GS (0, 2.5, 5, or 10 μ g/mL) for various periods of time prior to harvest.

2.10. Quantitative real-time RT-PCR (qRT-PCR)

Total RNA from cultured cells was extracted with TRIzol reagent and cDNA was synthesized using a PrimeScript RT reagent kit. Relative mRNA quantification was analyzed using a CFX96 Touch Real-Time PCR Detection System (Bio-Rad, Hercules, CA, USA) with settings as follows: initial denaturation at 95 °C for 5 min followed by 40 cycles of 95 °C for 15 s, 60 °C for 30 s, and 72 °C for 30 s. Relative cDNA levels were calculated using the 2^{- $\Delta\Delta$ Ct} method after normalization to GAPDH transcript levels. Primer sequences used for qRT-PCR are listed as follows: forward, 5'- TGA AGC CTA TGA

CAC CAC TGA -3' and reverse, 5'- TCC CCT ACG CTT TCT TGT CCT -3' for *FLG*; forward, 5'- TCC TCC AGT CAA TAC CCA TCA G -3' and reverse, 5'- CAG CAG TCA TGT GCT TTT CCT -3' for *IVL*; forward, 5'- CCT CCT GGG AGT GAT AGC AAT -3' and reverse, 5'- GGC AAC TAA AAT AGC CAG ACC T -3' for *Cldn-1*; forward, 5'-GGC CAT TGT TGA CCC CTA CA-3' and reverse, 5'- ATG GAG GTG CCA ATG ACC AG -3' for *AQP3*; forward, 5'- GTG AAG GTC GGA GTC AAC G -3' and reverse, 5'- TGA GGT CAA TGA AGG GGT C -3' for *GAPDH*.

2.11. Immunofluorescence staining

Cells were fixed in 4% paraformaldehyde for 15 min, permeabilized with 0.1% Triton X-100, and blocked in 5% BSA. Next, samples were incubated with primary antibodies (1:200) overnight at 4 °C followed by incubation with FITC-labeled goat anti-rabbit antibodies (1:100) for 1 h. Nuclei were stained with DAPI. Data pertaining to target protein localization and expression within cells were captured using a Cytation 5 cell imaging multifunctional test system (BioTek, Winooski, VT, USA).

2.12. Statistical analysis

Data were expressed as means \pm SD from three independent experiments. One-way analysis of variance (ANOVA) and Tukey's test were used to assess the significance of differences, with statistical analyses conducted using GraphPad Prism 7.0 (GraphPad Software, San Diego, CA, USA). $p < 0.05$ was considered statistically significant for all experiments.

3. Results

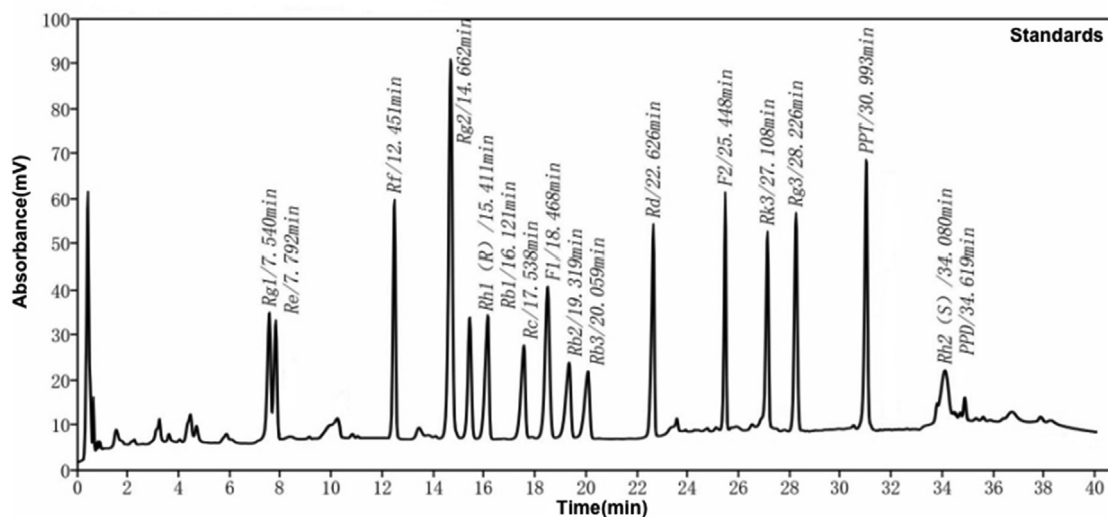
3.1. Ginsenoside composition of GS

GS monomeric contents were determined using a UPLC system, with relative proportions of monomeric constituents determined for each as follows: Rg1 (10.38%), Re (16.73%), Rf (4.25%), Rg2 (3.72%), Rh1(R) (0.22%), Rb1 (9.90%), Rc (8.27%), F1 (0.47%), Rb2 (7.62%), Rb3 (1.61%), Rd (13.36%), F2 (0.75%), Rk3 (1.64%), Rg3 (0.2%), PPT (1.4%), Rh2(S) (1.37%), and PPD (3.56%) (Fig. 1A and B). These 17 monomers accounted for 85.45% of GS content.

3.2. GS attenuated UVB-induced increase of epidermal thickness and TEWL and decrease of dorsal skin dehydration in BALB/c hairless mice

The results revealed no significant changes in body weights of mice in any groups regardless of treatment with or without GS (2.0 mg/cm²) (Fig. 2A). According to the experimental procedure (Fig. 2B), control skin exhibited a flat surface and showed no dryness, while obvious dryness and desquamation were observed in skin of mice directly exposed to UVB. As expected, the GS treatment group exhibited a low level of desquamation as well as a level of skin dryness resembling normal skin of the control group (Fig. 2C). Based on histological examination results (Fig. 2D), UVB irradiation markedly induced an increase in epidermal thickness by 1.62-fold relative to the control that was effectively reduced after topical GS application (Fig. 2E). As illustrated in Fig. 2F, the TEWL of the UVB-irradiated group increased by 1.47-fold compared with the control group, while the TEWL of the GS treatment group was significantly reduced as compared with the UVB + Vehicle group. Similarly, for TEWL results a 14-day topical application of GS could relieve the reduction in stratum corneum water content caused by UVB irradiation. Overall, our findings indicate that GS could effectively restore the physiological condition of the skin surface for

A



B

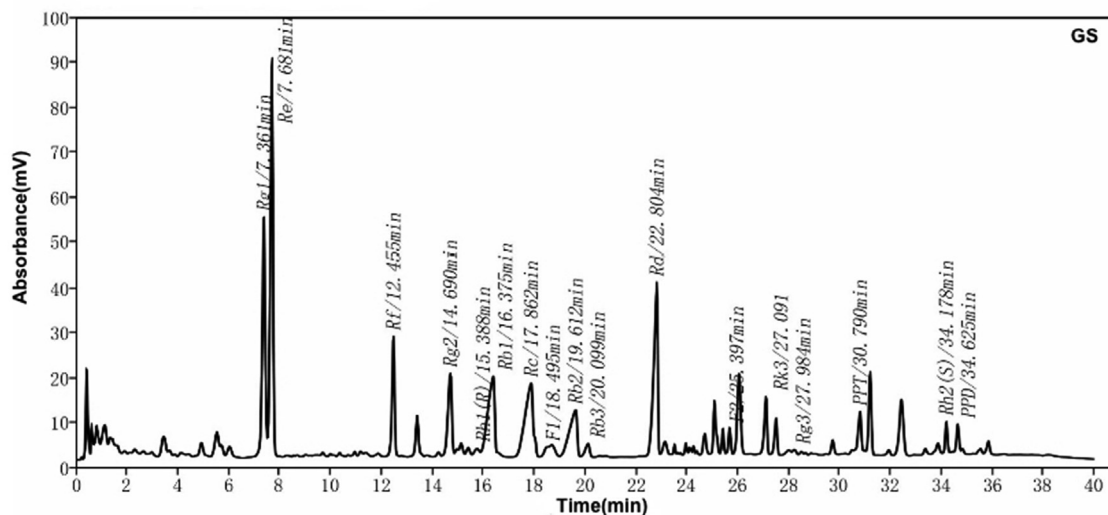


Fig. 1. Characterization of GS constituents by UPLC with UV detection at 203 nm. (A) UPLC chromatograms of standard ginsenosides. (B) UPLC chromatogram of GS.

increased protection against UVB-induced mice skin barrier damage.

3.3. GS increased FLG and IVL protein expression in UVB-irradiated BALB/c hairless mice

The results demonstrated that GS treatment could improve epidermal distributions of FLG and IVL after their levels were decreased by UVB irradiation, with FLG and IVL re-localizing to the epidermis after GS treatment to eventually reestablish their normal distributions (Fig. 3A and B). As compared with the control group, downregulated expression of both FLG and IVL proteins was observed in mouse epidermal skin after UVB irradiation, with GS treatment leading to significant upregulation of expression of these two proteins (Fig. 3C and D). These results suggest that GS normalized CE protein expression levels that were reduced after

UVB exposure, thereby restoring the normal distribution of skin mechanical barrier CE proteins to normal levels.

3.4. GS improved expression and localization of Cldn-1 in UVB-irradiated BALB/c hairless mice

To evaluate effects of GS treatment (2.0 mg/cm²) on regulation of Cldn-1 expression, we analyzed Cldn-1 expression and localization in skin tissues of GS-treated mice. Although Cldn-1 was found to be localized primarily in all living layers of the epidermis prior to UVB irradiation, after continuous UVB irradiation, Cldn-1 level decreased and was detected only in sparse quantities in the upper stratum basale. However, after GS treatment, Cldn-1 expression was restored to normal levels and the protein was found to be distributed throughout the entire epidermal layer (Fig. 3A–D). These results indicate that topical application of GS can

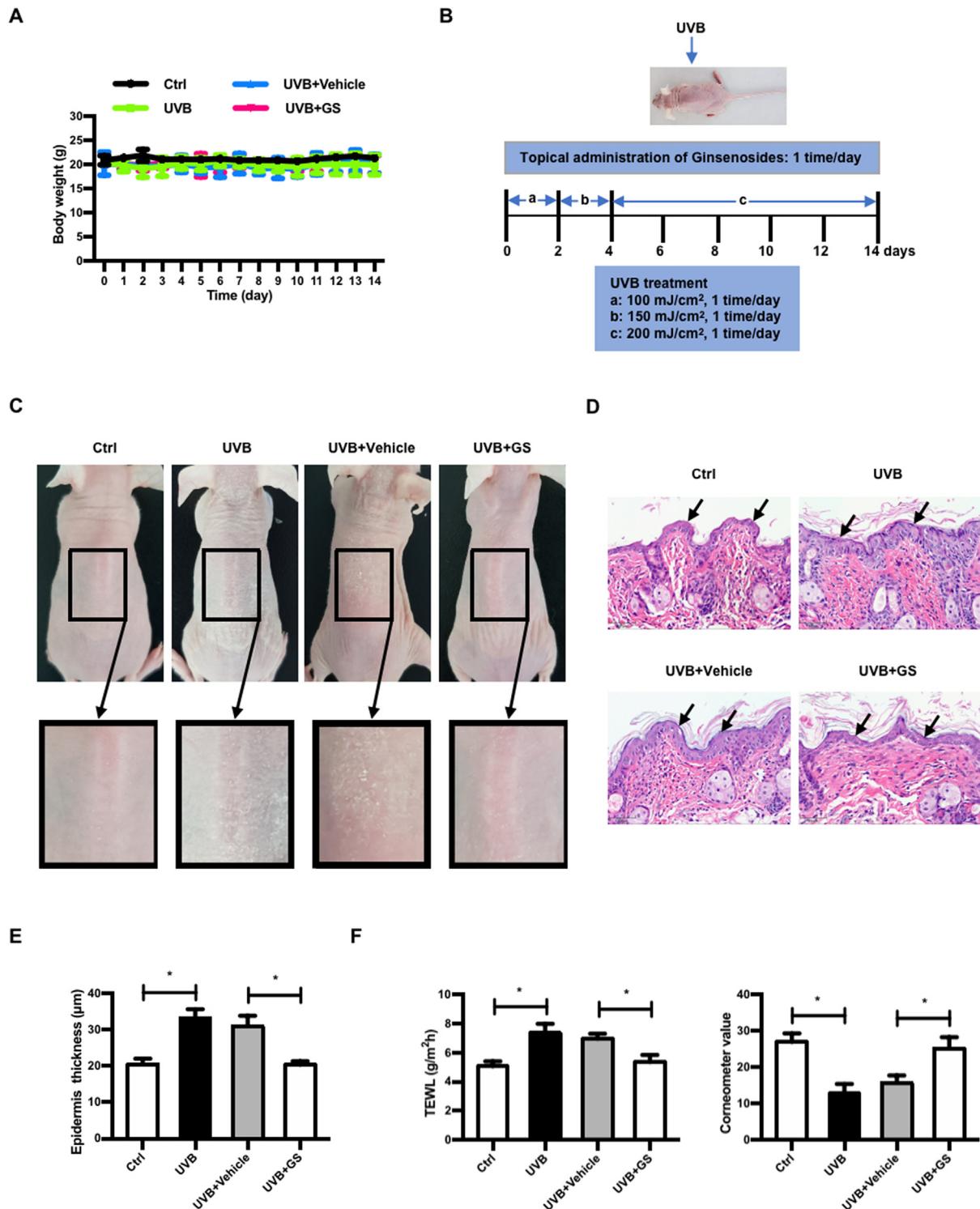


Fig. 2. Effect of topical application of GS on UVB-induced skin barrier damage of hairless mice for 2 weeks. (A) Body weight changes. (B) Schematic diagram of the animal experiment. (C) Representative images of dorsal skin surfaces exposed to UVB as described in (A). (D) Representative micrographs of H&E-stained skin tissue sections. Scale bar = 50 µm. Arrows indicate epidermal thickness. (E) Histogram of epidermal thickness of dorsal skin. (F) TEWL and stratum corneum water content of dorsal skin surfaces. Values are expressed as means ± SD (n = 5). *p < 0.05 vs. the control or UVB + Vehicle group.

restore both Cldn-1 level and localization pattern that ultimately lead to repair of impaired skin barrier TJ structure and function.

3.5. GS enhanced expression of AQP3 protein in UVB-irradiated BALB/c hairless mice

AQP3 expression determined immunohistochemically in tissues was found to be decreased in skin of UVB-irradiated group mice as

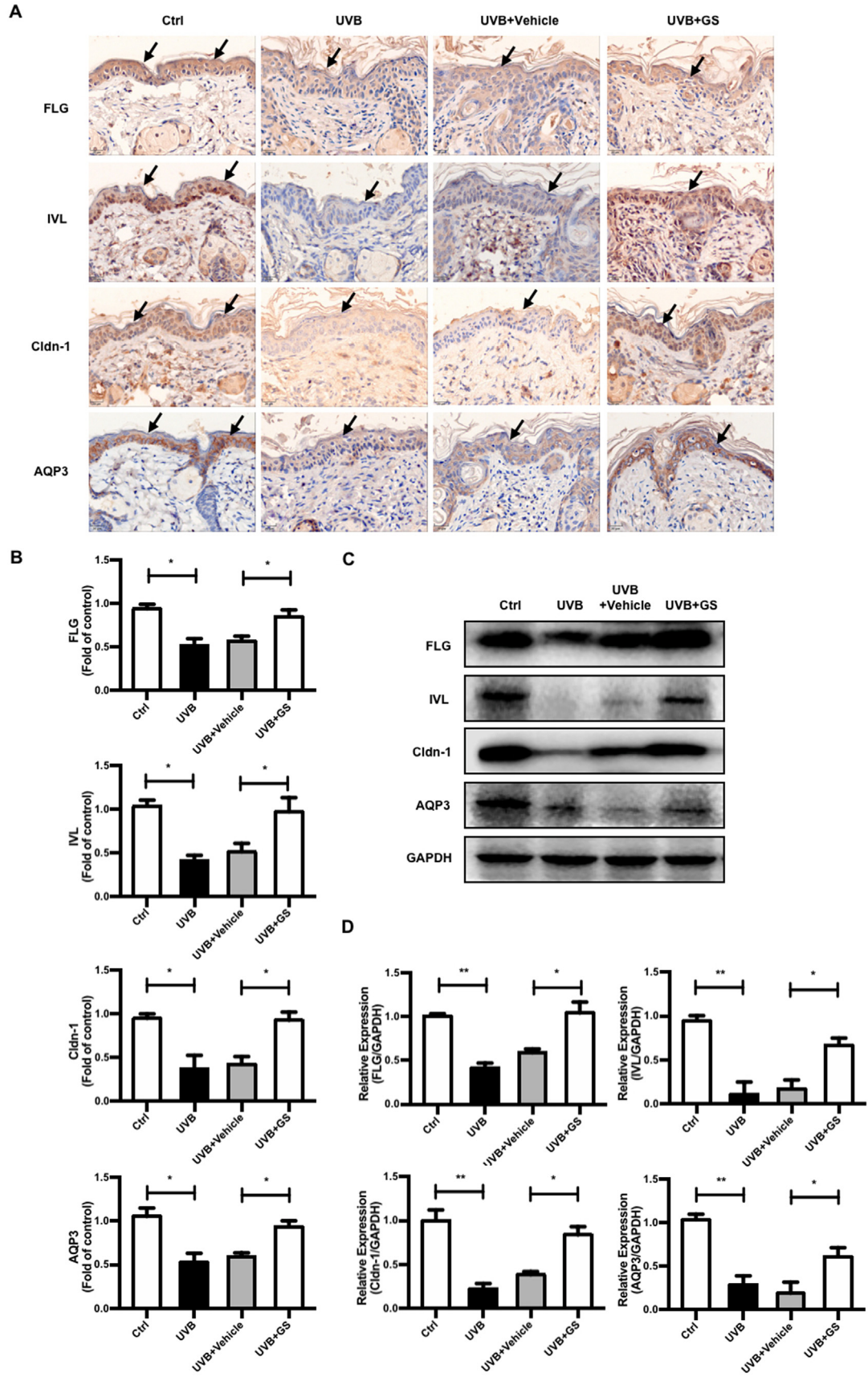


Fig. 3. Effect of topical application of GS on expression levels of CE, TJ, and AQP3 proteins in dorsal skin of UVB-irradiated mice. (A) Immunohistochemistry was conducted to monitor the FLG, IVL, Cldn-1, and AQP3 expression levels. Scale bar = 20 μ m. Arrows indicate location of mouse epidermis. (B) Immunohistochemical staining density analysis of

above proteins was shown, respectively. (C) Protein levels of FLG, IVL, Cldn-1, and AQP3 in dorsal skin of UVB-irradiated mice were analyzed by Western blot. (D) Relative expression levels of these proteins were quantified by densitometry analyses. GAPDH antibody was used as loading control. Values are expressed as means ± SD (n = 5). *p < 0.05 vs. the control or UVB + Vehicle group.

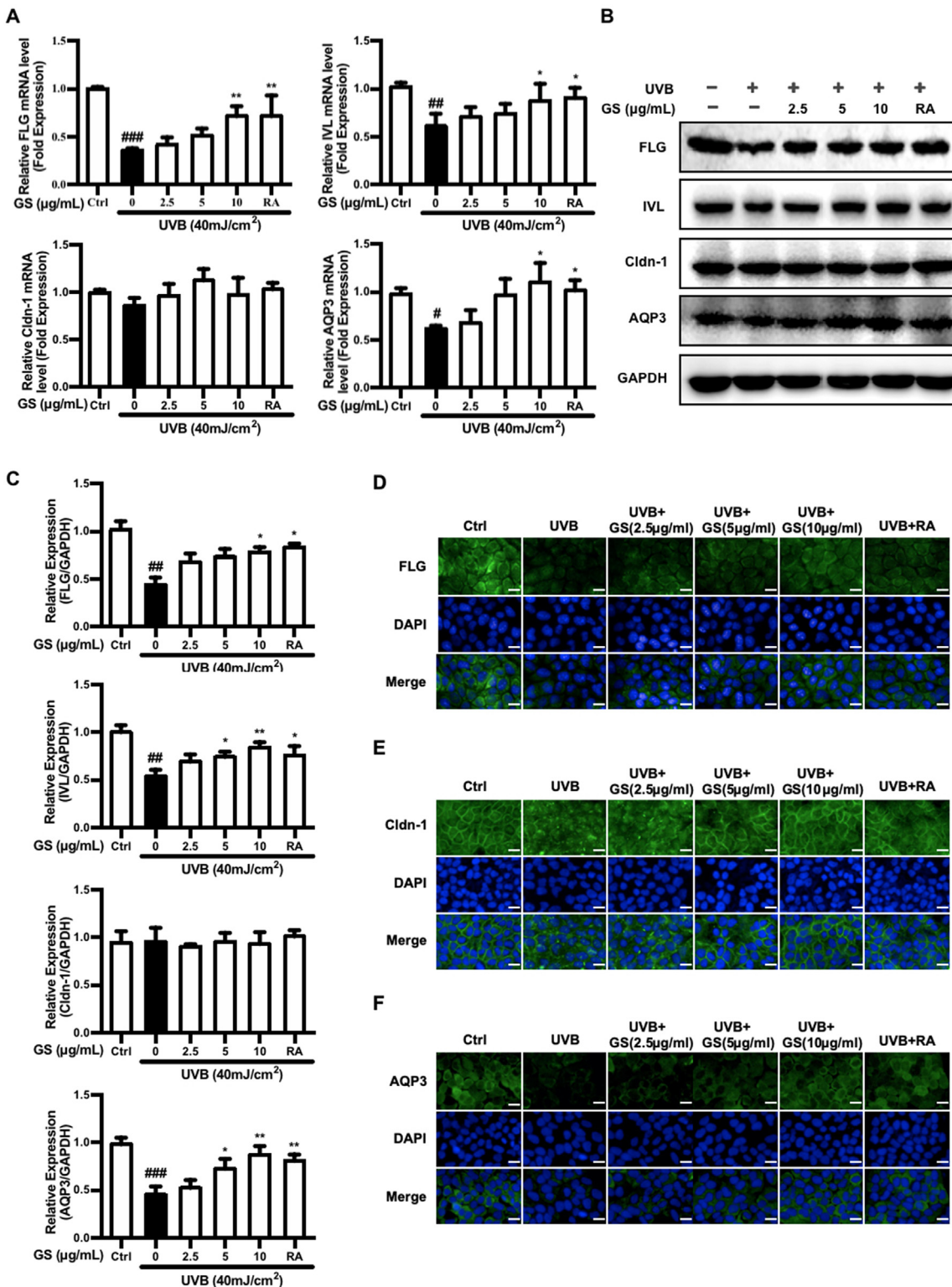


Fig. 4. Effects of GS treatment on UVB-exposed HaCaT cells. (A) The mRNA levels of FLG, IVL, Cldn-1 and AQP3 were assessed and quantified by qRT-PCR after GS treatment for 15 min. GAPDH mRNA expression was detected as the loading control. (B) After treatment of GS for 24 h, protein levels of FLG, IVL, Cldn-1, and AQP3 were analyzed by Western blot. (C) Relative expression levels of these proteins were quantified by densitometry analyses. GAPDH antibody was used as loading control. (D) Representative images of FLG, Cldn-1, and AQP3 staining were examined using a Cytation 5 cell imaging multifunctional test system. Scale bar = 20 µm. Values are expressed as means ± SD (n = 3). #p < 0.05, ##p < 0.01, ###p < 0.001 vs. the control group; *p < 0.05, **p < 0.01 vs. the UVB-irradiated group.

compared to the control group and was upregulated by GS treatment (2.0 mg/cm²) (Fig. 3A and B), as confirmed by Western blot results (Fig. 3C and D). Our data thus indicate that GS significantly inhibited UVB-induced skin dryness by upregulating AQP3 expression.

3.6. GS improved mRNA and protein expression of FLG, IVL, and AQP3 in UVB-irradiated HaCaT cells

As indicated in Fig. 4A–C, FLG, IVL, and AQP3 mRNA and protein expression levels were markedly attenuated in UVB-irradiated cells, while GS treatment (2.5, 5, 10 µg/mL) could effectively recover expression of FLG, IVL, and AQP3 in a dose-dependent manner. Indeed, a GS concentration of 10 µg/mL exerted almost the same effect as did the positive control treatment retinoic acid (RA). Immunofluorescence imaging further demonstrated higher quantities and more pervasive FLG and AQP3 protein distributions, especially in cytoplasm and cell membranes of the GS-treated UVB-irradiated group as compared to the untreated UVB-irradiated group (Fig. 4D and F). These data demonstrate that GS treatment protected against UVB-induced cutaneous barrier deterioration by upregulating expression of CE and AQP3 proteins *in vitro*.

3.7. GS restored Cldn-1 distribution in UVB-irradiated HaCaT cells

Normally, Cldn-1 is largely localized within apical regions of lateral membranes. After UVB irradiation, the tight junctional localization of Cldn-1 significantly decreased but was subsequently restored after GS treatment (2.5, 5, 10 µg/mL) in a dose-dependent manner (Fig. 4E). Notably, GS treatment restored Cldn-1 distribution in spite of the lack of detectable changes in Cldn-1 mRNA and protein expression levels as compared to respective RA group levels (Fig. 4A–C). These results show that GS could repair HaCaT cell damage caused by UVB irradiation by restoring normal TJ protein distribution.

3.8. GS decreased MAPK pathway activation in UVB-irradiated HaCaT cells

In our experiments, UVB irradiation resulted in increased phosphorylation of JNK, P38, and ERK. Compared to the UVB-irradiated group, treatment with GS at a concentration of 10 µg/mL significantly inhibited phosphorylation of MAPK pathway members JNK, P38, and ERK and exerted the same effects as observed for the RA-treated group. However, total JNK, P38, and ERK expression levels were unaffected by UVB irradiation with or without GS treatment (Fig. 5A and B). Accordingly, these data suggest that GS treatment suppressed JNK, P38, and ERK activation that subsequently prevented UVB-induced downregulation of FLG, IVL, AQP3 expression in HaCaT cells.

3.9. Identification of the active ginsenoside monomers in GS

To test which GS constituents had protective effects, 17 ginsenoside monomers were added to UVB-irradiated HaCaT cells in quantities corresponding to their proportions in GS as determined from UPLC analysis (Fig. 1). The results demonstrated that Rg2, Rg3, Rk3, F2, Rd, and Rb3 were jointly responsible for upregulation of IVL and AQP3 expression levels (Fig. 6A). Furthermore, treatment with the six-monomer mixture (GSM) markedly increased IVL and AQP3 protein levels to levels observed with GS treatment (Fig. 6B). Moreover, our studies have shown that GSM (the concentration of

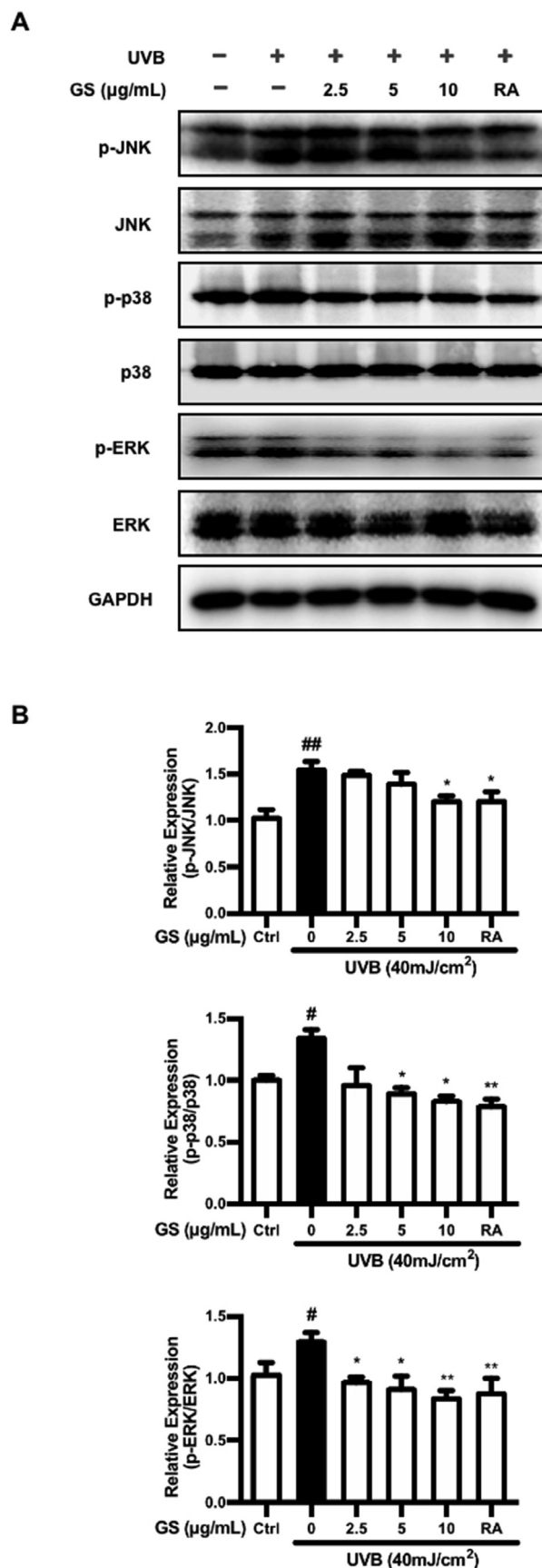


Fig. 5. Effects of GS treatment on MAPK signaling pathways in UVB-exposed HaCaT cells. (A) HaCaT cells were irradiated with UVB (40 mJ/cm²) and then treated with GS

(0, 2.5, 5, and 10 $\mu\text{g}/\text{mL}$) for 2 h. Phosphorylation status of MAPKs were analyzed by Western blot. (B) Relative expression levels of p-JNK/JNK, p-p38/p38, and p-ERK/ERK were quantified by densitometry analyses. GAPDH antibody was used as loading control. Values are expressed as means \pm SD ($n = 3$). # $p < 0.05$, ## $p < 0.01$ vs. the control group; * $p < 0.05$, ** $p < 0.01$ vs. the UVB-irradiated group.

GSM is equivalent to that in GS concentrations of 2.5, 5 and 10 $\mu\text{g}/\text{mL}$ also inhibited activation of the MAPK signaling pathway to enable repair of skin barrier damage (Fig. 6C and D). Therefore, data obtained here strongly suggest that GSM may contain most of the active components of GS responsible for restoring a healthy skin barrier after UVB damage.

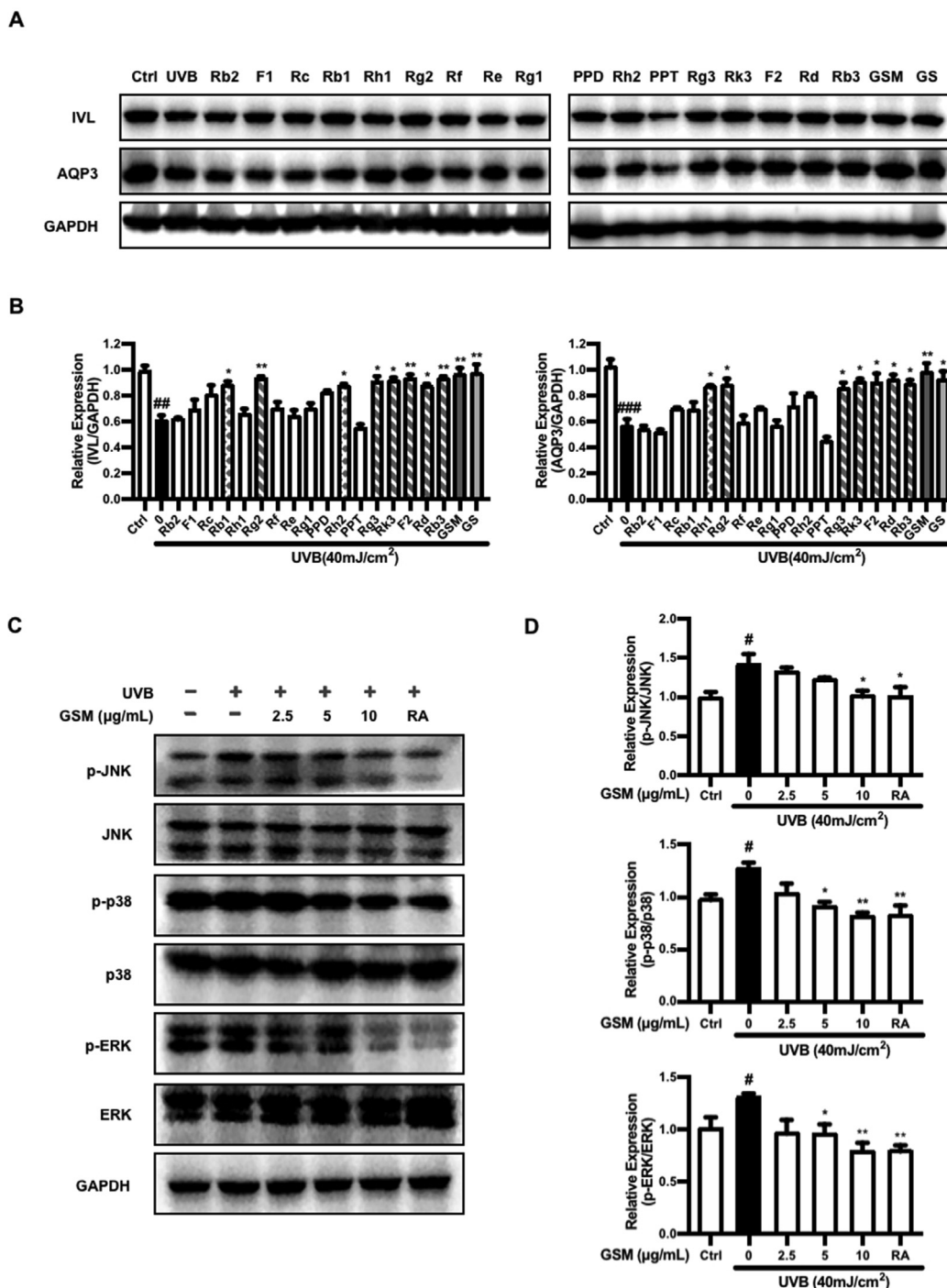


Fig. 6. Effects of GS ginsenoside monomers in the treatment of UVB-exposed HaCaT cells. (A) HaCaT cells were irradiated with UVB (40 mJ/cm²) then treated with GS ginsenoside monomers, GSM, or GS for 24 h. Protein levels of IVL and AQP3 were analyzed by Western blot. The composition of various monomers in GS is shown as Fig. 1. (B) Relative expression levels of IVL and AQP3 were quantified by densitometry analyses. (C) HaCaT cells were irradiated with UVB (40 mJ/cm²) and then treated with GSM (0, 2.5, 5, and 10 $\mu\text{g}/\text{mL}$) for 2 h. Phosphorylation status of MAPKs were analyzed by Western blot. (D) Relative expression levels of p-JNK/JNK, p-p38/p38, and p-ERK/ERK were quantified by densitometry analyses. GAPDH antibody was used as loading control. Values are expressed as means \pm SD ($n = 3$). # $p < 0.05$, ## $p < 0.01$, ### $p < 0.001$ vs. the control group; * $p < 0.05$, ** $p < 0.01$ vs. the UVB-irradiated group.

4. Discussion

P. ginseng has been used in China and other Asian countries for thousands of years due to its whitening [21], skin hydration [22], and anti-photoaging effects [15]. At present, aberrant changes in skin barrier structure and composition are considered to form the basis of many skin conditions and diseases, such as atopic dermatitis and ichthyosis. It had been previously reported that Re enhanced CE formation [16] and compound K treatment could augment FLG expression under physiological conditions [17]. Moreover, Rc promoted expression of CE-related proteins [18], while oral Rg1 intake could reduce mouse skin TEWL in the UVB-irradiated barrier disruption model [19]. Here we found that GS treatment led to repair of skin barrier damage caused by UVB exposure both *in vivo* and *in vitro*. This study is of great significance for revealing protective efficacy and active ingredients of ginseng against skin barrier damage.

Studies have shown that externally applied UVB irradiation to the skin causes epidermal changes such as dryness, desquamation, and hyperkeratosis [23]. As our results demonstrated, UVB-damaged skin barrier keratinocytes were shed from skin surfaces quickly, resulting in dry and rough skin, increased epidermal thickness, and weak water-trapping ability. TEWL, an indicator of skin barrier damage, increased after skin barrier damage; the increase in TEWL was accompanied by a decrease in skin hydration value (an indicator of skin water content), a result which is consistent with previously reported results [24–26]. In the present study, topical GS application onto skin could effectively reduce dryness and desquamation of mouse dorsal skin due to increased TEWL and decreased hydration value. Histological examination further revealed that after UVB irradiation, increased nucleated keratinocytes (hyperkeratosis) caused mouse skin tissue to thicken, leading to increased SC dryness and elevated TEWL that led to poor stratum corneum water content. These findings indicate that GS treatment exerted a macroscopically visible repair effect on the skin barrier.

Our research has demonstrated that UVB irradiation may reduce skin barrier function by reducing accumulation of barrier proteins FLG and IVL and by altering localization of TJ protein Cldn-1 and expression of AQP3. After GS treatment, expression levels of major barrier proteins FLG, IVL and AQP3 were significantly increased in a dose-dependent manner both *in vivo* and *in vitro*. Moreover, localization of FLG, IVL, Cldn-1, and AQP3 to the epidermis was restored and an absence of Cldn-1 within lower epidermal layers was observed that was significantly correlated with increased cell proliferation in UVB-damaged barrier skin, as reported previously [27–29]. In normal keratinocytes, a continuous networked Cldn-1 structure could be seen along the plasma membrane, while in UVB-irradiated keratinocytes Cldn-1 exhibited diffuse and fragmented dot-line expression. These findings indicate that keratinocytes irradiated by UVB lost the ability to form mature TJs, as characterized by a discontinuous membrane expression pattern of TJ protein [30,31]. After GS treatment, Cldn-1 network expression was restored and was followed by repair of TJ structural integrity. However, Cldn-1 mRNA and protein level expression in HaCaT keratinocytes did not change, as reported previously in UVB-irradiated rat epidermal keratinocytes (REKs) and normal human epidermal keratinocytes [32,33]. Therefore, this result may reflect UVB-induced internalization of Cldn-1, which neither changed the total Cldn-1 level nor altered phosphorylation of Cldn-1 level, although it did increase both Cldn-1 mono-ubiquitination and tyrosine nitration levels [34,35]. The present findings suggest that GS treatment could counteract UVB-induced impairments of skin barrier function by restoring expression and localization of key skin barrier proteins.

For epidermal keratinocytes, a variety of extracellular stimuli, including ultraviolet light, can trigger stress-related signal cascades, the most significant of which is the activation of MAPKs [36,37]. Signals sent through MAPKs can be subdivided into three main cascades that involve JNK and p38, which can be activated by a series of environmental stress factors, and ERK, which usually transmits signals from growth factors or mitogens. After these kinases are activated, they regulate transcription of various target proteins within the intracellular structure. Many studies have shown that MAPK pathway kinases are involved in disintegration of epithelial and endothelial junctions and in localization and accumulation of TJ within keratinocytes. The expression of AQP3 is also regulated by a MAPK pathway [38]. In this study, we found that GS markedly suppressed UVB-induced phosphorylation of JNK, p38, and ERK. Therefore, the GS protective role may restore expression of barrier-related proteins through inhibition of the MAPK pathway.

Finally, we screened GS constituent monomers based on their relative concentrations and found that of 17 monomers isolated, Rg2, Rg3, Rk3, F2, Rd, and Rb3 could promote increases in IVL and AQP3 protein levels. Furthermore, the effect of a combination treatment containing these six monomers was equivalent to the effect obtained using intact GS, thus confirming that the above-mentioned six ginsenoside monomers comprised the most active GS components for protecting the skin barrier from UVB damage. Further study revealed that the ability of the six-monomer mixture to stimulate skin repair was associated with inhibition of MAPK pathway phosphorylation. Previous studies had reported that Re and Rc exerted effects on skin barrier function, although no protective effect was detected here when Re and Rc were administered at their corresponding concentrations as found in GS. These conflicting results might reflect the fact that concentrations of Re (1.67 $\mu\text{g/mL}$ vs. 1.77 μM) and Rc (0.83 $\mu\text{g/mL}$ vs. 0.77 μM) used in our study were much smaller than doses tested in previous studies (minimum concentrations of Re and Rc of 5 μM) [16,18]. Nevertheless, the activity level of GSM did not equal or exceed the sum of the activities of its individual monomeric constituents, a result that suggests that potential mutual resistance or inhibitory interactions between these six active saponin monomers may be occurring. In conclusion, total ginsenosides may protect against UVB-irradiated skin barrier damage *in vivo* and *in vitro* by acting on the MAPK signaling pathway, with skin protective activity mainly provided by six active ginsenoside components.

Declaration of competing interest

All authors have no conflicts of interest to declare.

Acknowledgments

This study was supported by the National Key Research and Development Program of China (No. 2017YFC1702106), National Natural Science Foundation of China (Nos. U20A20402 and U19A2013), Science and Technology Development Plan of Jilin Province, China (Nos. 20180201075YY and 20180101128JC).

References

- [1] Tanaka Y, Uchi H, Furue M. Antioxidant cinnamaldehyde attenuates UVB-induced photoaging. *J Dermatol Sci* 2019;96(3):151–8.
- [2] Kang MC, Yumnam S, Kim SY. Oral intake of collagen peptide attenuates ultraviolet B irradiation-induced skin dehydration *in vivo* by regulating hyaluronic acid synthesis. *Int J Mol Sci* 2018;19(11).
- [3] Hung CF, Chen WY, Aljuffali IA, Lin YK, Shih HC, Fang JY. Skin aging modulates percutaneous drug absorption: the impact of ultraviolet irradiation and ovariectomy. *Age (Dordr)*. 2015;37(2):21.

- [4] Basler K, Bergmann S, Heisig M, Naegel A, Zorn-Kruppa M, Brandner JM. The role of tight junctions in skin barrier function and dermal absorption. *J Control Release* 2016;242:105–18.
- [5] Dang NN, Pang SG, Song HY, An LG, Ma XL. Filaggrin silencing by shRNA directly impairs the skin barrier function of normal human epidermal keratinocytes and then induces an immune response. *Braz J Med Biol Res* 2015;48(1):39–45.
- [6] Lee CW, Lin ZC, Hu SC, Chiang YC, Hsu LF, Lin YC, Lee IT, Tsai MH, Fang JY. Urban particulate matter down-regulates filaggrin via COX2 expression/PGE2 production leading to skin barrier dysfunction. *Sci Rep* 2016;6:27995.
- [7] Boivin FJ, Schmidt-Ott KM. Transcriptional mechanisms coordinating tight junction assembly during epithelial differentiation. *Ann N Y Acad Sci* 2017;1397(1):80–99.
- [8] Brandner JM. Importance of tight junctions in relation to skin barrier function. *Curr Probl Dermatol* 2016;49:27–37.
- [9] Tang SC, Tang LC, Liu CH, Liao PY, Lai JC, Yang JH. Glycolic acid attenuates UVB-induced aquaporin-3, matrix metalloproteinase-9 expression, and collagen degradation in keratinocytes and mouse skin. *Biochem J* 2019;476(10):1387–400.
- [10] Kwon KR, Alam MB, Park JH, Kim TH, Lee SH. Attenuation of UVB-induced photo-aging by polyphenolic-rich *Spatholobus suberectus* stem extract via modulation of MAPK/AP-1/MMPs signaling in human keratinocytes. *Nutrients* 2019;11(6).
- [11] Choi HJ, Alam MB, Baek ME, Kwon YG, Lim JY, Lee SH. Protection against UVB-induced photoaging by *Nyssa fruticans* via inhibition of MAPK/AP-1/MMP-1 signaling. *Oxid Med Cell Longev* 2020;2020:2905362.
- [12] Myung DB, Han HS, Shin JS, Park JY, Hwang HJ, Kim HJ, Ahn HS, Lee SH, Lee KT. Hydrangol isolated from the leaves of *hydrangea serrata* attenuates wrinkle formation and repairs skin moisture in UVB-irradiated hairless mice. *Nutrients* 2019;11(10).
- [13] Kang HJ, Huang YH, Lim HW, Shin D, Jang K, Lee Y, Kim K, Lim CJ. Stereospecificity of ginsenoside Rg2 epimers in the protective response against UV-B radiation-induced oxidative stress in human epidermal keratinocytes. *J Photochem Photobiol B* 2016;165:232–9.
- [14] Hwang E, Park SY, Jo H, Lee DG, Kim HT, Kim YM, Yin CS, Yi TH. Efficacy and safety of enzyme-modified Panax ginseng for anti-wrinkle therapy in healthy skin: a single-center, randomized, double-blind, placebo-controlled study. *Rejuvenation Res* 2015;18(5):449–57.
- [15] Kim YH, Park HR, Cha SY, Lee SH, Jo JW, Go KH, Lee SY, Shin SS. Effect of red ginseng NaturalGEL on skin aging. *J Ginseng Res* 2020;44(1):115–22.
- [16] Oh Y, Lim HW, Kim K, Lim CJ. Ginsenoside Re improves skin barrier function in HaCaT keratinocytes under normal growth conditions. *Biosci Biotechnol Biochem* 2016;80(11):2165–7.
- [17] Kim E, Kim D, Yoo S, Hong YH, Han SY, Jeong S, Jeong D, Kim JH, Cho JY, Park J. The skin protective effects of compound K, a metabolite of ginsenoside Rb1 from Panax ginseng. *J Ginseng Res* 2018;42(2):218–24.
- [18] Oh Y, Lim HW, Park KH, Huang YH, Yoon JY, Kim K, Lim CJ, Kim K. Ginsenoside Rc protects against UVB-induced photooxidative damage in epidermal keratinocytes. *Mol Med Rep* 2017;16(3):2907–14.
- [19] Jimbo N, Kawada C, Nomura Y. Herb extracts and collagen hydrolysate improve skin damage resulting from ultraviolet-induced aging in hairless mice. *Biosci Biotechnol Biochem* 2015;79(10):1624–8.
- [20] Ren X, Shi Y, Zhao D, Xu M, Li X, Dang Y, Ye X. Naringin protects ultraviolet B-induced skin damage by regulating p38 MAPK signal pathway. *J Dermatol Sci* 2016;82(2):106–14.
- [21] Kim K. Effect of ginseng and ginsenosides on melanogenesis and their mechanism of action. *J Ginseng Res* 2015;39(1):1–6.
- [22] Lee JO, Kim E, Kim JH, Hong YH, Kim HG, Jeong D, Kim J, Kim SH, Park C, Seo DB. Antimelanogenesis and skin-protective activities of Panax ginseng calyx ethanol extract. *J Ginseng Res* 2018;42(3):389–99.
- [23] Peng Z, Chen B, Zheng Q, Zhu G, Cao W, Qin X, Zhang C. Ameliorative effects of peptides from the oyster (*Crassostrea hongkongensis*) protein hydrolysates against UVB-induced skin photodamage in mice. *Mar Drugs* 2020;18(6).
- [24] Han HS, Shin JS, Myung DB, Ahn HS, Lee SH, Kim HJ, Lee KT. *Hydrangea serrata* (thunb.) ser. Extract attenuate UVB-induced photoaging through MAPK/AP-1 inactivation in human skin fibroblasts and hairless mice. *Nutrients* 2019;11(3).
- [25] Tokudome Y, Masutani N, Uchino S, Fukai H. Recovery effects of oral administration of glucosylceramide and beet extract on skin barrier destruction by UVB in hairless mice. *Nutrients* 2017;9(11).
- [26] Wang PW, Cheng YC, Hung YC, Lee CH, Fang JY, Li WT, Wu YR, Pan TL. Red raspberry extract protects the skin against UVB-induced damage with anti-oxidative and anti-inflammatory properties. *Oxid Med Cell Longev* 2019;2019:9529676.
- [27] Hung CF, Fang CL, Al-Suwayeh SA, Yang SY, Fang JY. Evaluation of drug and sunscreen permeation via skin irradiated with UVA and UVB: comparisons of normal skin and chronologically aged skin. *J Dermatol Sci* 2012;68(3):135–48.
- [28] Jin SP, Han SB, Kim YK, Park EE, Doh EJ, Kim KH, Lee DH, Chung JH. Changes in tight junction protein expression in intrinsic aging and photoaging in human skin in vivo. *J Dermatol Sci* 2016;84(1):99–101.
- [29] Gruber R, Bornchen C, Rose K, Daubmann A, Volksdorf T, Wladykowski E, Vidal-y-Sy S, Peters EM, Danso M, Bouwstra JA. Diverse regulation of claudin-1 and claudin-4 in atopic dermatitis. *Am J Pathol* 2015;185(10):2777–89.
- [30] Kojima T, Fuchimoto J, Yamaguchi H, Ito T, Takasawa A, Ninomiya T, Kikuchi S, Ogasawara N, Ohkuni T, Masaki T. c-Jun N-terminal kinase is largely involved in the regulation of tricellular tight junctions via tricellulin in human pancreatic duct epithelial cells. *J Cell Physiol* 2010;225(3):720–33.
- [31] Jia Z, Wang X, Wang X, Wei P, Li L, Wu P, Hong M. Calycosin alleviates allergic contact dermatitis by repairing epithelial tight junctions via down-regulating HIF-1 α . *J Cell Mol Med* 2018;22(9):4507–21.
- [32] El-Chami C, Haslam IS, Steward MC, O'Neill CA. Organic osmolytes preserve the function of the developing tight junction in ultraviolet B-irradiated rat epidermal keratinocytes. *Sci Rep* 2018;8(1):5167.
- [33] Yuki T, Hachiya A, Kusaka A, Sriwiriyanont P, Visscher MO, Morita K, Muto M, Miyachi Y, Sugiyama Y, Inoue S. Characterization of tight junctions and their disruption by UVB in human epidermis and cultured keratinocytes. *J Invest Dermatol* 2011;131(3):744–52.
- [34] Kobayashi M, Shu S, Marunaka K, Matsunaga T, Ikari A. Weak ultraviolet B enhances the mislocalization of claudin-1 mediated by nitric oxide and peroxynitrite production in human keratinocyte-derived HaCaT cells. *Int J Mol Sci* 2020;21(19).
- [35] Marunaka K, Kobayashi M, Shu S, Matsunaga T, Ikari A. Brazilian green propolis rescues oxidative stress-induced mislocalization of claudin-1 in human keratinocyte-derived HaCaT cells. *Int J Mol Sci* 2019;20(16).
- [36] Chen F, Tang Y, Sun Y, Veeraraghavan VP, Mohan SK, Cui C. 6-shogaol, a active constituents of ginger prevents UVB radiation mediated inflammation and oxidative stress through modulating Nrf2 signaling in human epidermal keratinocytes (HaCaT cells). *J Photochem Photobiol B* 2019;197:111518.
- [37] Jo K, Bae GY, Cho K, Park SS, Suh HJ, Hong KB. An anthocyanin-enriched extract from vaccinium uliginosum improves signs of skin aging in UVB-induced photodamage. *Antioxidants (Basel)* 2020;9(9).
- [38] Tang SC, Tang LC, Liu CH, Liao PY, Lai JC, Yang JH. Glycolic acid attenuates UVB-induced aquaporin-3, matrix metalloproteinase-9 expression, and collagen degradation in keratinocytes and mouse skin. *Biochem J* 2019;476(10):1387–400.